Crystal Growth

Deutsche Ausgabe: DOI: 10.1002/ange.201603794
Internationale Ausgabe: DOI: 10.1002/anie.201603794

Realignment of Nanocrystal Aggregates into Single Crystals as a Result of Inherent Surface Stress

Zhaoming Liu, Haihua Pan, Genxing Zhu, Yaling Li, Jinhui Tao, Biao Jin, and Ruikang Tang**

Abstract: *Crystallization by particle attachment is widely observed in both natural and synthetic environments. Although this form of nonclassical crystallization is generally described by oriented attachment, random aggregation of building blocks to give single-crystal products is also observed, but the mechanism of crystallographic realignment is unknown. We herein reveal that random attachment during aggregation-based growth initially produces a nonoriented growth front. Subsequent evolution of the orientation is driven by the inherent surface stress applied by the disordered surface layer and results in single-crystal formation by grain-boundary migration. This mechanism is corroborated by measurements of orientation rate versus external stress, which demonstrated a predictive relationship between the two. These findings advance our understandings about aggregation-based growth via nanocrystal blocks and suggest an approach to material synthesis that takes advantage of stress-induced coalignment.*

Aggregation-based crystal growth (AG), which occurs by the aggregation and coalescence of nanoparticles rather than by ion-by-ion attachment, has been widely observed in the field and laboratory.[1] Typically, the resulting material can be identified as single crystal by diffraction techniques.[2] A number of studies proposed that this kind of structure forms through oriented attachment (OA), that is, the addition of nanocrystals with identical or twin-related crystallographic alignments.[3]

Recently, in situ transmission electron microscopy (TEM) in a liquid cell was used to directly show that nanocrystals made several attempts to attach before they found a perfect lattice match, after which they became irreversibly fused in an oriented manner.[3a] Despite clear proof for the existence of OA, the achievement of perfect crystallographic alignment between crystalline blocks over large dimensions is likely to be difficult in general.[4] There is extensive evidence for the involvement of distinct polymorphs during crystal growth, thus eliminating the possibility of the direct coalignment of building blocks.[5] Moreover, random attachment (RA) rather than OA during crystal growth has also been directly observed, despite the fact that, in both cases, the products are still single crystals.[6] The mechanism that allows these misaligned crystals and/or polymorphs to transition into single crystals during RA-based crystal growth is unclear.[1e,5d,6a] Herein, we demonstrate that the inherent stress applied on the disordered surface layer is the driving force for the evolution of crystal orientation during RA, thus resulting in the formation of a bulk single crystal through grain-boundary migration.

Calcium carbonate ($CaCO_3$) was used as the model system for investigating the evolution of crystal orientation during AG because it is the most abundant rock-forming mineral and biomineral in nature, and has been reported to grow by either AG or classical crystal-growth mechanisms.[3d,7] In our experiment, a mixed solvent (ethanol/water, v/v 9:1) was used as the reaction medium to switch from the classical crystallization pathway to AG. The high-ethanol-content system reduced the solubility of $CaCO_3$, thus reducing the possibility of dissolution–reprecipitation competing with AG (see the Supporting Information). When CO_2 gas was bubbled into $Ca(OH)_2$ solutions, $CaCO_3$ nanocrystallites were rapidly formed (within 1 min).

The initially formed particles in the reaction solution had a typical size of (8 ± 2) nm (Figure 1 a,f), and they were identified as the vaterite phase by X-ray diffraction (see Figure S3 in the Supporting Information). The use of these nanocrystals as the building blocks for crystal growth resulted in the formation of a final spindle-shaped vaterite single crystal (Figure 1 a–e, 1 h; see also Figures S4 and S5). The crystal-growth process was also monitored in situ under a fluorescence microscope (see the Supporting Information), which confirmed the AG pathway. The grain features on the surface of the final vaterite crystal were identified by scanning electron microscopy (SEM; see Figure S6) and atomic force microscopy (AFM; see Figure S7), and the results supported our conclusion that the final vaterite crystal resulted from aggregation of the initial vaterite nanoparticles.

High-resolution TEM (HRTEM) showed that the thin surface layer of each crystal actually consisted of disordered nanocrystals, as seen from lattice-fringe images and fast Fourier transform (FFT) patterns (Figure 1 g; see also Figure S8). These disordered nanocrystals were similar to the initial nanocrystals in the solution (Figure 1 f). In contrast, sensitive selected-area electron diffraction (SAED) showed typical single-crystal-like features in the crystal bulk (Figure 1 h). Ultrathin section images from the surface to the bulk (Figure 1 i–k) revealed the structural evolution. The polycrystalline surface layer was thin and had a typical thickness of 5–

[*] Z. Liu, G. Zhu, Y. Li, B. Jin, Prof. R. Tang
Department of Chemistry, Zhejiang University
Hangzhou, Zhejiang 310027 (China)
E-mail: rtang@zju.edu.cn
Dr. H. Pan, Prof. R. Tang
Qiushi Academy for Advanced Studies, Zhejiang University
Hangzhou, Zhejiang 310027 (China)
E-mail: panhh@zju.edu.cn
Dr. J. Tao
Physical Sciences Division, Pacific Northwest National Laboratory
Richland, WA 99354 (USA)

Supporting information for this article can be found under: http://dx.doi.org/10.1002/anie.201603794.

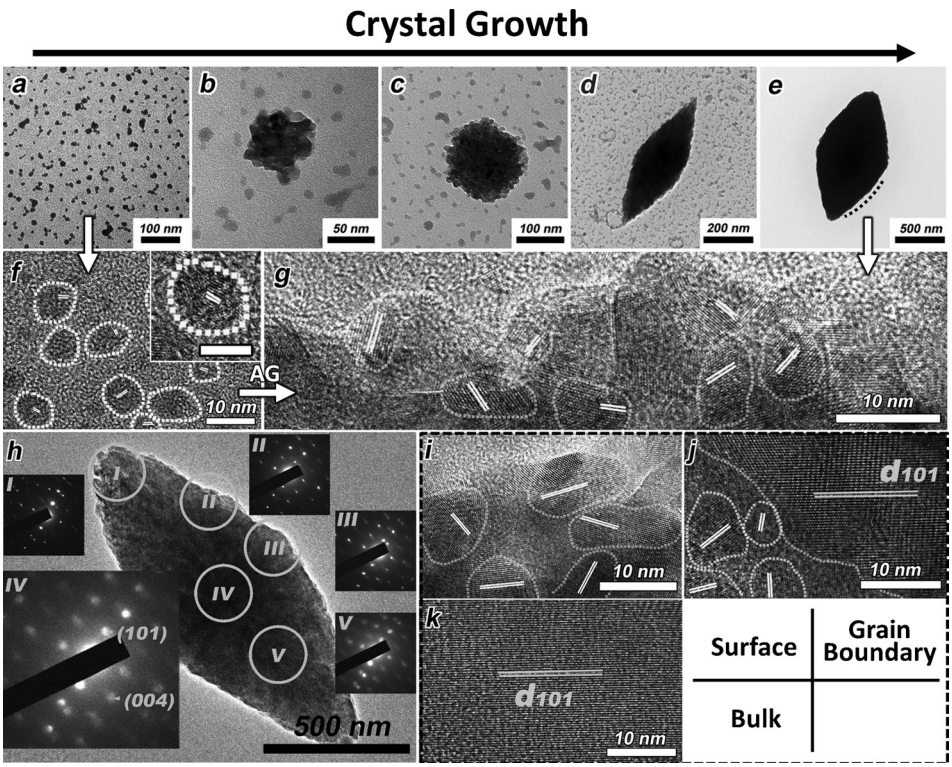

Figure 1. Characterization of the AG of vaterite. a–e) TEM images showing that nanocrystals served as building blocks for the final spindle-shaped vaterite crystal. During this process, the nanoparticles were formed first (a), followed by particle attachment to generate a vaterite sphere (b,c, <375 s). During crystal growth, spindle-shaped vaterite was formed (d, ca. 625 s). In the end, all nanocrystals were attached to spindle vaterite, and the background became clean (e, ca. 750 s). f) Initially formed nanoparticles with lattice fringes, indicating that the blocks were crystalline vaterite. Inset: higher-magnification image of a nanocrystal (scale bar: 5 nm). g) The surface of the final spindle vaterite (ca. 750 s) consisted of randomly aligned nanocrystals. Notably, the attached nanocrystals had a similar shape and size to those of the initial nanoparticles. h) The SAED of the spindle-shaped vaterite was the same as that of a single crystal of vaterite. i–k) Cross-section of a final spindle vaterite crystal showing the structure from the surface to the bulk: The surface layer contains nonoriented vaterite grains (i); the grain boundary between the bulk and nonoriented surface layer is indicated with a dotted line (j); the bulk is single-crystal vaterite (k).

20 nm (Figure 1j). Underneath that, the bulk phase was a perfect vaterite single crystal (Figure 1k). Higher-magnification TEM images showed grain boundaries between the bulk single-crystal vaterite and the nonoriented surface layer (Figure 1j), which does not show lattice matching or twin boundaries. Because the surface layer was only around 10 nm in thickness, its contribution to the SAED pattern (over the size of 200×200 nm^2) was minor, and therefore the patterns (Figure 1h) were dominated by diffraction from the underlying bulk vaterite single crystal instead of the disordered surface layer.

To understand the structural evolution during crystal growth, we used observations of lattice fringes to track order in the surface layer over time. Notably, the thickness of the polycrystalline surface layer did not increase, even though the vaterite crystals grew from nanometer-sized particles to micron-sized spindles. The thickness of polycrystalline surface remained in the range of a few to ten nanometers, thus showing that, as nanocrystals continually attached to the surface of the vaterite crystal, the underlying layer of misaligned blocks recrystallized to adopt the same orientation as that of the interior of the bulk crystal (Figure 2a–c). Moreover, owing to this reorganization, structural evidence for particle aggregation during formation of the bulk crystal was abolished.[5b,6b]

Figure 2d shows the typical steps of the approach, attachment, and fusion of nanocrystals to the surface of the bulk vaterite crystal. The crystalline structure of the unattached nanocrystals could be clearly observed from the lattice fringes (Figure 2d, I). When the nanocrystals attached to the surface of the main crystal, no lattice match was found at the interface between the two (Figure 2d, II). Even after the nanocrystal attached to the surface layer, no lattice match was observed (Figure 2d, III), thus demonstrating the RA pathway. The RA process generated a surface layer of vaterite nanoparticles with random orientations (Figure 2d, IV) surrounding the bulk crystal (Figure 2d, V). However, recrystallization occurred through movement of the grain boundaries, thus leading to the growth of bulk single-crystal vaterite. From these steps in the process, it follows that the growth front during RA consisted of a nonoriented nanometer-thick layer of vaterite, despite the fact that the bulk phase was a single crystal.

These findings demonstrate that underneath the randomly aggregated nanoparticle layer, realignment occurs; but what is the driving force? Previously, improvement of the orientation of crystals was generally understood to be an aging process driven by the dissolution of less stable particles, and it was thought that the incorporation of the growth units into stable particles was controlled by interfacial tension.[8] However, even after aging for 2 weeks at 25 °C, the outermost layer of vaterite spindles still remained in the disordered state without any realignment (Figure 3a). This result shows that the process of realignment is not a simple aging process.

After trying several ways to induce the evolution of crystal orientation in the surface layer, we discovered that the application of high pressure promoted realignment. We stored the final particles in a high-pressure environment (under nitrogen gas at a pressure of 2 MPa) at 25 °C (see Figure S9). After aging of the vaterite for 4 h, the outer shell exhibited the same orientation as that of the bulk (Figure 3b;

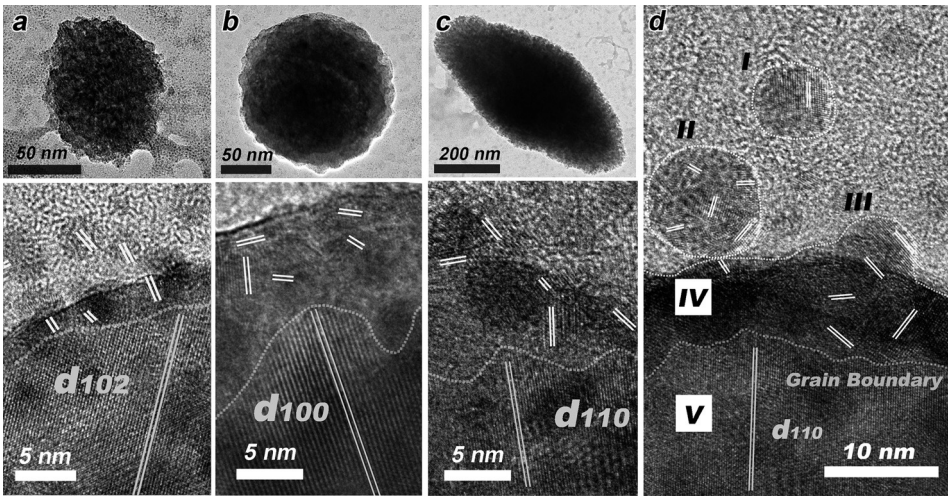

Figure 2. Evolution of crystal orientation in the vaterite bulk phase. a–c) The vaterite crystals always contained a 2–20 nm nonoriented surface layer during the crystal-growth process, and underneath the surface was the single-crystal bulk: a) 150 s, b) 300 s, c) 450 s. d) Attachment of nanocrystals onto the vaterite surface at an early stage (at 300 s): I) Individual nanoparticle; II) initial attachment of a nanocrystal without lattice matching; III) later stage of attachment of a nanocrystal with the spindle vaterite surface without lattice matching; IV) nonoriented surface layer; V) oriented bulk.

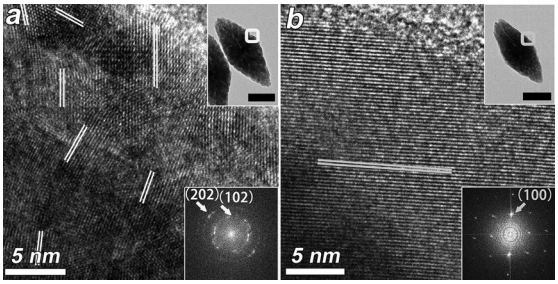

Figure 3. Stress-driven realignment of the surface layer. a) The surface layer still remained nonoriented after aging for 2 weeks, thus proving that realignment could not be simply understood as the result of aging. Top right: low-resolution TEM image of a vaterite spindle (scale bar: 500 nm); bottom right: fast Fourier transform (FFT) of the lattice-fringe image. b) The surface layer became oriented after aging at an external pressure of 2 MPa, thus supporting the hypothesis that the evolution of the crystal orientation process was driven by stress. Top right: low-resolution TEM image of a vaterite spindle (scale bar: 500 nm); bottom right: FFT of the lattice-fringe image.

see also Figure S10). We confirmed that surface realignment was not induced by dissolution of the nonoriented surface by performing a similar pressure experiment in pure ethanol (see Figure S11). This finding suggests that stress is the key to the realignment.

In the polycrystalline surface layer, grain boundaries separated the vaterite nanoparticles with different orientations (Figures 1j and 2), and no obvious gaps were found at these boundaries. Thus, we believed that recrystallization could only occur by grain-boundary migration, which has been widely observed in metallurgy and geology.[3a,9] Grain-boundary migration is equivalent to the growth of one crystallite at the expense of its receding neighbors. If this process were occurring in the vaterite crystals, it could eventually alter the orientation of grains underneath the surface layer to produce a single crystal.

Stress is known to be a driving force for grain-boundary migration (see the Supporting Information), and the effects of stress on realignment were seen in this study (Figure 3b).[9] In the absence of applied stress, the source of stress that leads to grain-boundary migration below the disordered surface layer can be understood by considering the inherent surface stress, σ_{surf}, of a nanoparticle of radius R, which is given by (see the Supporting Information):

$$\sigma_{surf} = \frac{8\gamma}{R} \quad (1)$$

in which R is the curvature of a vaterite spindle ($R \approx 20$–200 nm) and $\gamma = 40\ mJ\,m^{-2}$.[10] Equation (1) gives a σ_{surf} value of about 16–1.6 MPa.

Besides the inherent surface stress, the application of a hydrostatic external pressure from solution (p_{ex}) will be transferred to the grain boundaries through the outer shell. The total stress exerted (σ_{total}) can be expressed as (see the Supporting Information):

$$\sigma_{total} = p_{ex} + \sigma_{surf} \quad (2)$$

Because of the high stress produced by the surface layer (16–1.6 MPa), stress-driven migration of shell–bulk grain boundaries leads to the recrystallization of vaterite beneath the surface layer. However, the outer surface only receives stress from the external pressure (p_{ex}) of the atmosphere (0.1 MPa), which is ten times less than the stress experienced by the interior. Therefore, no realignment was observed in the outermost layer.

The rate, u, of stress-driven grain-boundary migration can be quantitatively expressed as a function of stress, σ, by the equation (see the Supporting Information):

$$u = av\, e^{-\frac{Q_0}{kT}} e^{\frac{av\Omega\sigma}{kT}} \left(1 - e^{-\frac{\Delta V\sigma}{kT}}\right) \quad (3)$$

in which a is the hopping lattice distance for diffusion; v is the Debye frequency; Q_0 is the diffusion barrier without stress; α is a positive nondimensional coefficient; ν is the Poisson ratio; Ω is the unit volume; and ΔV is the change in volume upon grain-boundary migration. As the grain boundary migrates outward from the bulk, the fraction, f, of oriented vaterite increases and is determined by the migration rate:

$$f = \frac{u}{d} \times t \quad (4)$$

in which d is the depth of the shell. Combining Equations (2–4) gives:

$$f = C(e^{\frac{Bp_{ex}}{kT}} - e^{\frac{(B-\Delta V)p_{ex}}{kT}})t \quad (5)$$

in which C, B, and ΔV are constants for a given particle size. The oriented fraction in the shell layer can be analyzed from HRTEM images (see the Supporting Information), and the parameters in Equation (5) can be obtained by calculating the slope of f versus t at different external pressures (Figure 4a; see also Figure S12). From our data, we obtain $C = 0.0059\ h^{-1}$, $B = 1.1 \times 10^{-26}\ m^3$, and $\Delta V = 4.0 \times 10^{-27}\ m^3$ (Figure 4b). With these parameters, the realignment of the surface layer at any given external pressure and time can be predicted, and these predictions were corroborated by our experiments (Figure 4c).

The findings reported above show that vaterite forms through AG by random attachment followed by the evolution of the crystal orientation pathway. Moreover, they reveal the mechanism underlying the realignment process and confirm the driving force for realignment (Figure 4d). In general, the reorganization of randomly attached crystallites (nonoriented attachment) requires that huge barriers are overcome, as demonstrated by the high external pressure required for realignment of the outer layer in our experiments. However, the surface layer of randomly aggregated nanoparticles naturally generates a high surface stress, which is sufficient to induce the evolution of crystal orientation in the inner region of the crystal. This surface stress is the driving force for the recrystallization of polycrystalline aggregates to form well-oriented bulk single crystals.

By uncovering the evolution of the crystal orientation process and its mechanism, we hope to advance our understanding of both the natural formation and laboratory synthesis of minerals by AG. AG that appears to occur through OA or nearly oriented attachment may coexist with AG through RA, followed by stress-induced crystallization (e.g. the growth of akaganeitie, hematite, anatase, rutile, and goethite).[1a,f,6b] Most of these systems have been assumed to pass through an OA process, without any direct observation of such a process. Crystal growth in some porous media, such as collagen fibrils, may be induced by capillary action as a result of stress-driven alignment.[11] Furthermore, this finding suggests an approach to materials synthesis that takes advantage of stress-induced coalignment, which could improve the performance of materials. More generally, understanding of stress-driven realignment during nanoparticle attachment provides a strategy for orientation control and grain-boundary reconstruction in crystal engineering, and paves the way to the rational design of materials with controlled orientation.

Acknowledgements

We thank James De Yoreo and Jennifer Soltis for helpful discussions. We also thank Qiaohong He for TEM assistance. This research was supported by the Fundamental Research Funds for the Central Universities (2012XZZX005) and the National Natural Science Foundation of China (No. 21571155). The AFM measurements were supported by the US Department of Energy (DOE), Office of Basic Energy Sciences, Division of Chemical Sciences, Geosciences, and Biosciences and were performed at Pacific Northwest National Laboratory, which is a multiprogram national laboratory operated by Battelle for the US DOE under Contract DE-AC05-76RL01830.

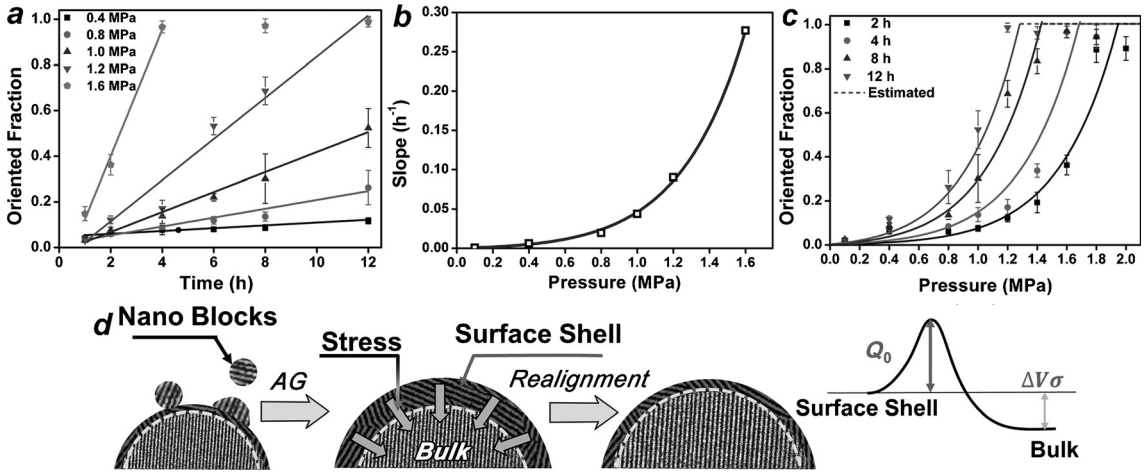

Figure 4. Stress-driven realignment process. a) Under external pressure, the fraction of oriented vaterite in the surface layer increased with time. Higher stress promoted the evolution of the crystal orientation process. Symbols are experimental data points, and lines are fitting results. b) The fitting of Equation (5) represents the relationship between the slopes of the plots in (a) and external pressure. By fitting, the parameters B, C, and ΔV in Equation (5) were determined. c) Predictions of oriented fractions for a range of external pressures and times on the basis of Equation (5). Symbols are experimental data points, and lines are results calculated by Equation (5). d) Schematic illustration of the process of random attachment followed by realignment. Nanocrystals attach randomly to the surface of a vaterite crystal to form a polycrystalline surface shell on the bulk. The outer surface shell inherently generates a high surface stress, which is sufficient to induce realignment in the inner region of the crystal. Crystal growth of the bulk (realignment process) occurs by grain-boundary migration, which needs to overcome a diffusion barrier, Q_0. The stress, σ, is the driving force for realignment.

Keywords: aggregation · calcium carbonate · crystal growth · crystal orientation · surface stress

How to cite: *Angew. Chem. Int. Ed.* **2016**, *55*, 12836–12840
Angew. Chem. **2016**, *128*, 13028–13032

[1] a) J. F. Banfield, S. A. Welch, H. Z. Zhang, T. T. Ebert, R. L. Penn, *Science* **2000**, *289*, 751–754; b) Y. Yin, A. P. Alivisatos, *Nature* **2005**, *437*, 664–670; c) W. J. Habraken, J. Tao, L. J. Brylka, H. Friedrich, L. Bertinetti, A. S. Schenk, A. Verch, V. Dmitrovic, P. H. Bomans, P. M. Frederik, J. Laven, P. van der Schoot, B. Aichmayer, G. de With, J. J. De Yoreo, N. A. Sommerdijk, *Nat. Commun.* **2013**, *4*, 1507; d) A. Dey, P. H. Bomans, F. A. Müller, J. Will, P. M. Frederik, G. de With, N. A. Sommerdijk, *Nat. Mater.* **2010**, *9*, 1010–1014; e) J. J. De Yoreo, P. U. Gilbert, N. A. Sommerdijk, R. L. Penn, S. Whitelam, D. Joester, H. Zhang, J. D. Rimer, A. Navrotsky, J. F. Banfield, A. F. Wallace, F. M. Michel, F. C. Meldrum, H. Cölfen, P. M. Dove, *Science* **2015**, *349*, aaa6760.

[2] a) T. X. Wang, H. Cölfen, M. Antonietti, *J. Am. Chem. Soc.* **2005**, *127*, 3246–3247; b) A. N. Kulak, P. Iddon, Y. Li, S. P. Armes, H. Cölfen, O. Paris, R. M. Wilson, F. C. Meldrum, *J. Am. Chem. Soc.* **2007**, *129*, 3729–3736; c) X. Fei, W. Li, Z. Shao, S. Seeger, D. Zhao, X. Chen, *J. Am. Chem. Soc.* **2014**, *136*, 15781–15786.

[3] a) D. Li, M. H. Nielsen, J. R. I. Lee, C. Frandsen, J. F. Banfield, J. J. De Yoreo, *Science* **2012**, *336*, 1014–1018; b) R. L. Penn, J. F. Banfield, *Science* **1998**, *281*, 969–971; c) H. Cölfen, M. Antonietti, *Angew. Chem. Int. Ed.* **2005**, *44*, 5576–5591; *Angew. Chem.* **2005**, *117*, 5714–5730; d) H. Cölfen, M. Antonietti, *Mesocrystals and Nonclassical Crystallization*, Wiley, West Sussex, **2008**.

[4] Y.-Y. Kim, A. S. Schenk, J. Ihli, A. N. Kulak, N. B. J. Hetherington, C. C. Tang, W. W. Schmahl, E. Griesshaber, G. Hyett, F. C. Meldrum, *Nat. Commun.* **2014**, *5*, 4341.

[5] a) E. M. Pouget, P. H. H. Bomans, J. A. C. M. Goos, P. M. Frederik, G. de With, N. A. J. M. Sommerdijk, *Science* **2009**, *323*, 1455–1458; b) J. Mahamid, A. Sharir, L. Addadi, S. Weiner, *Proc. Natl. Acad. Sci. USA* **2008**, *105*, 12748–12753; c) N. T. K. Thanh, N. Maclean, S. Mahiddine, *Chem. Rev.* **2014**, *114*, 7610–7630; d) Y. Politi, T. Arad, E. Klein, S. Weiner, L. Addadi, *Science* **2004**, *306*, 1161–1164; e) J. Mahamid, B. Aichmayer, E. Shimoni, R. Ziblat, C. Li, S. Siegel, O. Paris, P. Fratzl, S. Weiner, L. Addadi, *Proc. Natl. Acad. Sci. USA* **2010**, *107*, 6316–6321; f) M. Kerschnitzki, A. Akiva, A. B. Shoham, Y. Asscher, W. Wagermaier, P. Fratzl, L. Addadi, S. Weiner, *J. Struct. Biol.* **2016**, *195*, 82–92.

[6] a) H.-G. Liao, L. Cui, S. Whitelam, H. Zheng, *Science* **2012**, *336*, 1011–1014; b) M. H. Nielsen, D. Li, H. Zhang, S. Aloni, T. Han, C. Frandsen, J. Seto, J. F. Banfield, H. Cölfen, J. J. De Yoreo, *Microsc. Microanal.* **2014**, *20*, 425–436.

[7] a) G. Nancollas, M. Reddy, *J. Colloid Interface Sci.* **1971**, *37*, 824–830; b) H. H. Teng, P. M. Dove, J. J. De Yoreo, *Geochim. Cosmochim. Acta* **2000**, *64*, 2255–2266; c) J. W. Morse, R. S. Arvidson, A. Lüttge, *Chem. Rev.* **2007**, *107*, 342–381.

[8] F. Natalio, T. P. Corrales, M. Panthöfer, D. Schollmeyer, I. Lieberwirth, W. E. Müller, M. Kappl, H.-J. Butt, W. Tremel, *Science* **2013**, *339*, 1298–1302.

[9] a) G. Gottstein, L. S. Shvindlerman, *Grain Boundary Migration in Metals*: *Thermodynamics*, *Kinetics*, *Applications*, CRC, Boca Raton, **2009**; b) C. Passchier, R. Trouw in *Microtectonics*, Springer, Berlin, Heidelberg, **1998**, pp. 131–151.

[10] F. Manoli, E. Dalas, *J. Cryst. Growth* **2000**, *218*, 359–364.

[11] a) F. Nudelman, K. Pieterse, A. George, P. H. Bomans, H. Friedrich, L. J. Brylka, P. A. Hilbers, G. de With, N. A. Sommerdijk, *Nat. Mater.* **2010**, *9*, 1004–1009; b) Y.-Y. Kim, N. B. J. Hetherington, E. H. Noel, R. Kroeger, J. M. Charnock, H. K. Christenson, F. C. Meldrum, *Angew. Chem. Int. Ed.* **2011**, *50*, 12572–12577; *Angew. Chem.* **2011**, *123*, 12780–12785.

Received: April 19, 2016
Revised: May 31, 2016
Published online: July 19, 2016

